Journal of Physics: Conference Series

Design of an optical biosensor based on photonic crystal at THz frequency

Journal of Physics: Conference Series **1567** (2020) 022017 doi:10.1088/1742-6596/1567/2/022017

Design of an optical biosensor based on photonic crystal at THz frequency

T P Negara

Computer Science Division, Faculty of Mathematic and Natural Science, Universitas Pakuan, Bogor

Corresponding author: teguhpuja795@gmail.com

Abstract. We discuss the transmission characteristics of photonic crystal with two defect illuminated by a continuous wave of Transverse Electric (TE) mode at low terahertz frequency. To study its performance we solve numerically the corresponding Maxwell equations by means of finite difference frequency domain method. By varying the angle of incident, width of defect layer and refractive index in the second defect layer, it is found that the device exhibits a significant transmission enhancement at two wavelengths with typical changes. We also demonstrate its potential applications for biosensor platform

1. Introduction

The periodic structure or photonic crystal is an object to be continuously studied because many phenomena can be utilized for optical devices. The emergence of photonic band gap (PBG) phenomena in periodic structures without defects [1] and the emergence of photonic band pass (PBP) phenomena in periodic structures with defects [2] has been widely used for wavelength filters [3] and sensors [4]. For the wavelength range of visible light, periodic structures with defects have been successfully studied showing optical characteristics that can be utilized as a solution sensor [5]. For periodic metal-dielectric structures, a Surface Plasmon Resonance (SPR) phenomenon has been shown which can increase the intensity of the field around the metal layer and dielectric because there is a coupling of a surface plasmon with electromagnetic fields around the metal-dielectric surface. [6]. Theoretically, the propagation of electromagnetic waves at THz frequency causes the localized surface mode of the plasmon to be stronger, which is then called the Spoof Surface Plasmon Polaritons (SSPP) [7]. SSPP will not appear on flat metal surfaces at low frequencies because the skin depth of the metal is ignored at this frequency [8].

Simulations on photonic crystal with one metal defect layers, performed using the Finite Difference Frequency Domain (FDFD) method. The use of the FDFD method has several reasons. First, all materials have complex permittivity and permeability that are frequency dependent. Second, this method may be the simplest of all methods to implement and is excellent for field visualization and for developing new ways to model devices. Third, flexibility in calculating a single frequency or a few frequencies, generating responses from multiple shots using a direct solver, or implementation of an elasticity by directly introducing complex constitutive relations [9]. The purpose of this simulation is to analyze changes in the physical and optical properties of structures when light is transmitted to the structure. Simulation results show that changes in optical parameters such as the angle of incidence can shift PBP at certain wavelengths, while variations in the refractive index of the second defect layer can adjust the peak of PBP that can be directed to optical biosensors.

2. Photonic Crystal

Photonic crystal (PC) are periodical optical micro- and nanostructures that receive increasing attention due to their ability to manipulate light propagation while maintaining high transmission efficiency [10]. If electromagnetic waves propagate into the photonic crystal structure, then the waves will be scattered due to differences in the refractive index in the structure. If the wavelength, is much greater than the lattice constant of the PC, the structure behaves like an effective medium, but if the wavelength is proportional or smaller than the lattice constant of the PC there will be a Bragg reflection, thus forming a PBG in each boundary field of two different dielectric materials [11]. An important property of photonic crystal can be obtained if there is a defect in the photonic crystal structure. The defect causes localization around the band gap so that only transmittance will occur at one or a certain frequency intervals known as photonic passband [12]. PC are now being developed for sensors [13] and biosensors [14]. Photonic crystal-based biomaterials have advantages in the multiplex detection, biomolecular screening, and real-time monitoring of biomolecules. In addition, photonic crystal provide good platforms for drug loading and biomolecule modification, which could be applied to biosensors and biological carriers [15].

Photonic crystal structure reviewed as in figure 1, consists of layers TiO_2 and $GaAs$ arranged alternately with the refractive index respectively 2.78 and 3.61, then inserted two layers of defects, the gold layer Au with the refractive index $0.27732 + 2.9278i$ and a receptor layer that can be filled with material to be sensed. The optical length of the layer meets the quarter wave stack conditions, which are: $n_1 d_1 = \lambda_0 / 4$ and $n_2 d_2 = \lambda_0 / 4$ while the defect layer d_{d1} and d_{d2} can be varied in the simulation test. The angle of incident θ from electromagnetic waves concerning structures can be varied to regulate the position of PBP at certain operational wavelength used is $150 \mu m$

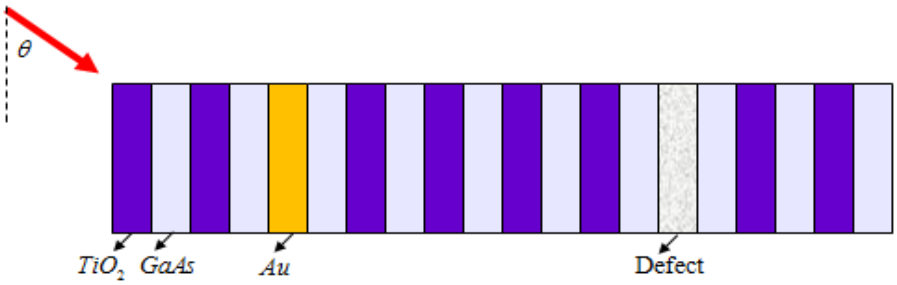

Figure 1. Design of a photonic crystal structure with two defect layers

3. FDFD Formulation

Maxwell's equation for $\boldsymbol{E}$ and $\boldsymbol{H}$ field can be written in the frequency domain after substitution and normalized as [16]:

$$\nabla \times \boldsymbol{E} = k_0 \mu \boldsymbol{H} \tag{1}$$

$$\nabla \times \boldsymbol{H} = k_0 \varepsilon \boldsymbol{E} \tag{2}$$

The discretization of Maxwell's equations for TE mode can be written

$$\frac{\partial \boldsymbol{E}_y}{\partial x'} - \frac{\partial \boldsymbol{E}_x}{\partial y'} = \frac{\boldsymbol{E}_y^{-i+1,j} - \boldsymbol{E}_y^{-i,j}}{\Delta x'} - \frac{\boldsymbol{E}_x^{-i,j+1} - \boldsymbol{E}_x^{-i,j}}{\Delta y'} = \mu_{zz} \boldsymbol{H}_z^{i,j} \tag{3}$$

$$\frac{\partial \boldsymbol{H}_z}{\partial y'} = \frac{\boldsymbol{H}_z^{i,j} - \boldsymbol{H}_z^{i,j-1}}{\Delta y'} = \varepsilon_{xx} \boldsymbol{E}_x^{i,j} \tag{4}$$

$$-\frac{\partial \boldsymbol{H}_z}{\partial x'} = -\frac{\boldsymbol{H}_z^{i,j} - \boldsymbol{H}_z^{i-1,j}}{\Delta x'} = \varepsilon_{yy} \boldsymbol{E}_y^{i,j} \tag{5}$$

The discrete equation can be formed into an Eigen equation, which is [16].

$$k_0^2 \boldsymbol{H}_z = \left\{ \varepsilon_{12}^{-1} U_1 \varepsilon_{33}^{-1} V_2 - \varepsilon_{22}^{-1} U_1 \varepsilon_{33}^{-1} V_1 \right\} \boldsymbol{H}_z \tag{6}$$

By applying boundary conditions Bloch can be used to get a matrix U and V, then the equation can be written:

$$A_H \boldsymbol{H}_z = 0 \tag{7}$$

Transmittance can be generated through the solution of the Eigen equation formed from a matrix A, field source f_{src}, and masking matrix Q

$$T_H(m) = \left| S_{trn}(m) \right|^2 . \left[\frac{k_{z,m}^{trn}}{k_z^{inc}} \frac{\varepsilon_{ref}}{\varepsilon_{trn}} \right] \tag{8}$$

4. Result and Discussion

The simulation results at the Figure 2 show the existence of two PBP at certain wavelengths. The position of PBP can be adjusted by changing the angle of incidence of the structure as shown in Figure 2. Simulation on the thickness of the defect layer $d_{d1} = d_{d2} = 2\lambda_0 / 7$ and angle incident 0^0 generate PBP at wavelength $302.845\,\mu m$ and $399.796\,\mu m$. When the angle is varied 30^0 (blue), 45^0 (green), and 60^0 (black), then the PBP shifts towards smaller wavelengths accompanied by changes in the peak PBP. For biosensor applications, the wavelength can be adjusted to match the biomolecular resonance.

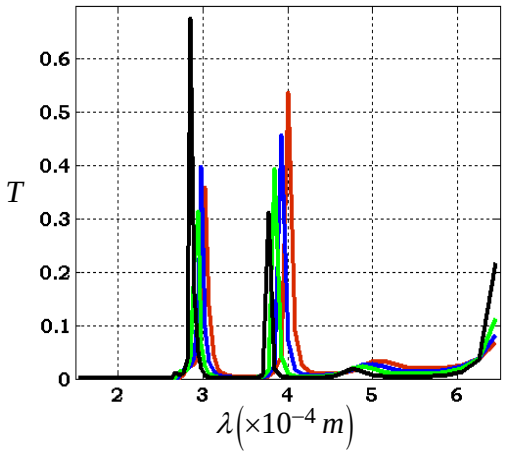

Figure 2. PBP shifts with angle incident variations: 0^0 (red), 30^0 (blue), 45^0 (green), and 60^0 (black)

The presence of a defect layer is a major factor in the emergence of PBP. The width of the first and second defect layers d_d can determine the peak of PBP. The effective width of the two defect layers

for the existence of PBP is from $0.222\lambda_0 - 0.286\lambda_0$. PBP Peak at wavelength $302.845\,\mu m$ ($0.75THz$) tend to be linear whereas PBP peak at wavelength $399.796\,\mu m$ ($0.99THz$) change non-linearly as the figure 3.

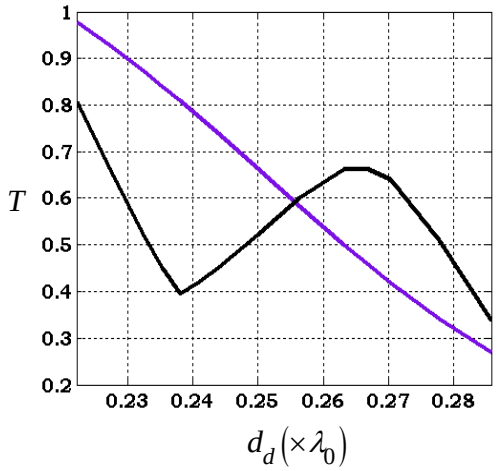

Figure 3. Changes in PBP peaks to changes in width of the first and second defect layers: PBP at wavelength $302.845\,\mu m$ (blue), and PBP at wavelength $399.796\,\mu m$ (black)

Changes in the material refractive index in the second defect layer can produce changes at the PBP peak. Figure 4 shows two PBP at wavelength $302.845\,\mu m$ (a) and $399.796\,\mu m$ (b) whose PBP peak changes accordingly to changes in the material refractive index, namely: 1.30,1.33,1.36, and 1.39. The response of PBP peak changes to changes in the refractive index of the material in this second defect layer can be developed for sensor devices by placing bio material in the second defect to be sensed.

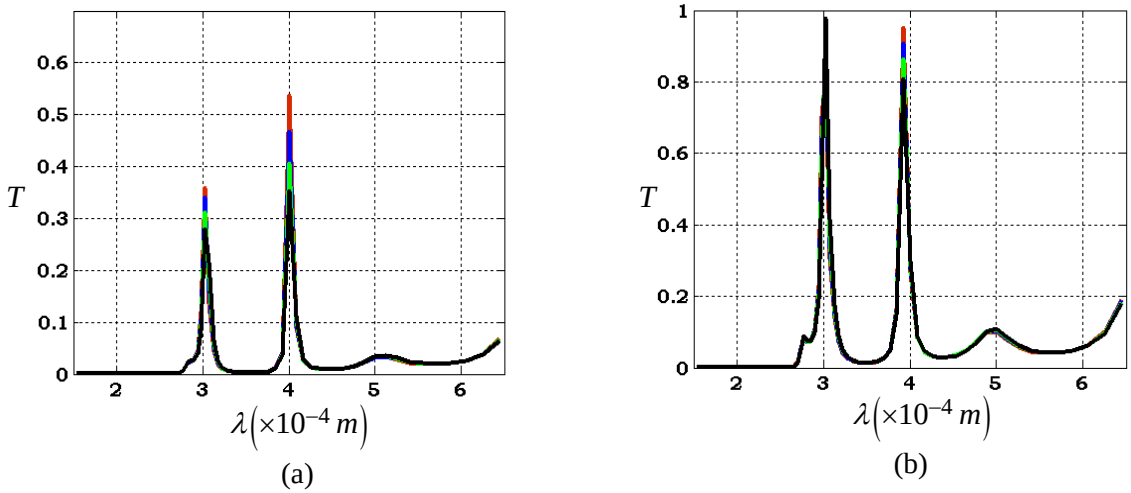

Figure 4. Photonic Passband response at wavelength $302.845\,\mu m$ and $399.796\,\mu m$ to changes in the material refractive index: 1.30 (red), 1.33 (blue), 1.36 (green), and 1.39 (black) with the width of the defect layer: (a) $2\lambda_0 / 7$ and (b) $2\lambda_0 / 9$

To see the response of changes in PBP peak to changes in the material refractive index can be seen in the Figure 5. At the thickness of the defect layer $2\lambda_0/7$, response to PBP changes at wavelength $302.845\,\mu m$ (a) and $399.796\,\mu m$ (b) have sensitivity respectively 2 and 0.9. While the defect layer $2\lambda_0/9$, response to PBP changes at wavelength $302.845\,\mu m$ and $399.796\,\mu m$ have sensitivity respectively 1.7 and 1.6. This good sensitivity value cannot be separated from the use of metal layer as the first defect which results in the SPR phenomenon between metal layers and dielectric layers.

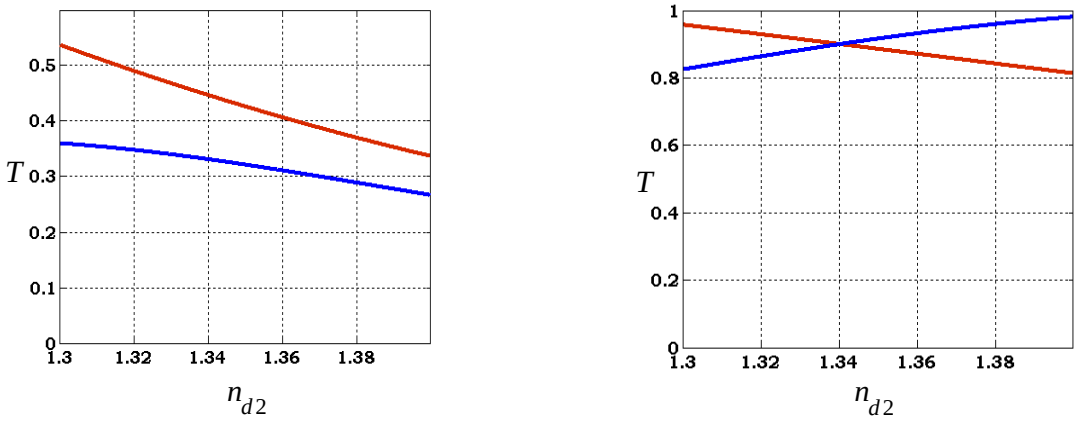

Figure 5. Response of the PBP to changes in the refractive index at wavelengths $302.845\,\mu m$ (red) and $399.796\,\mu m$ (blue) for width of the defect layer: (a) $0.222\lambda_0$ and (b) $0.286\lambda_0$

5. Conclusion

Photonic crystal design simulations with two defects have been analyzed using the FDFD method. The existence of a metal layer in the first defect and dielectric layer in the second defect causes the existence of two PBP at two wavelengths, namely: $302.845\,\mu m$ and $399.796\,\mu m$ or frequency equivalent $0.75THz$ and $0.99THz$. Changes in the angle of incidence can shift the position of PBP at the desired wavelength. The width of the first and second defect layers is set on the value $2\lambda_0/7 - 2\lambda_0/9$ with a maximum sensitivity of 2. These simulation values can be used as standards for the development of optical biosensor devices. For biosensor applications, the wavelength can be adjusted to resonate with biomolecular vibrations by adjusting the angle of incidence.

References

[1] Simsek S, Palaz S, Mamedov A M and Ozbay E 2017 *Appl. Phys. A* **123** 33
[2] Taymaz F K and Alireza B 2017 *Phys. Lett. A* **381** 38
[3] Parimal S and Bijoy K D 2018 *Appl. Optics* **57** 9
[4] Negara T P and Agung P 2019 *Int. J. Recent Tech. Eng (IJRTE)* **8** 2S7 33
[5] Ashour M A and Ahmed M 2019 *Sci. Rep.* **9** 6973
[6] Ilchenko SG, Lymarenko RA and Taranenko VB 2017 *Nanoscale Res. Lett.* **12** 295
[7] Ying Z, Yuehong X, Chunxiu T, Quan X, Xueqian Z, Yanfeng L, Xixiang Z, Jiaguang H and Weili Z 2017 *Opt. Express* **28** 13
[8] Xin G, Wenquan C and Wenjie F 2018 *Sci. Rep.* **8** 2456
[9] Na F, Lian F Z, Xiao B X and Zhen X Y 2018 *Geophysics* **83** 4
[10] Zhiyuan Y, Amitabh J, Rena K and Yuri R 2015 *J. Opt. Soc. Am. B* **32** 10
[11] Jing H, Yang C, Li X, Cao Z and Chen S 2018 *Photonic Res.* **6** 4
[12] Fang W, Yong Z C, Xiang W, Yi N Z, Yan N and Rong Z G 2018 *Materials* **11** 7

[13] Rajendran A, Thinakaran S and Savarimuthu R 2019 *Photonic Sensors* **9** 1
[14] Giampaolo P and Thomas F K 2018 *J. Optics* **20** 7
[15] Divya J, Sivanantharaja A and Selvendran S 2018 *Laser Physics* **28** 6
[16] Rumpf R C, Garcia C R, Berry E A and Barton J H 2014 *Prog, Electromagn. Res. B* **61**